Natural Hazards
and Earth System
Sciences

Global ground strike point characteristics in negative downward lightning flashes – Part 1: Observations

Dieter R. Poelman[1], Wolfgang Schulz[2], Stephane Pedeboy[3], Dustin Hill[4], Marcelo Saba[5], Hugh Hunt[6], Lukas Schwalt[7], Christian Vergeiner[7], Carlos T. Mata[4], Carina Schumann[6], and Tom Warner[8]

[1]Royal Meteorological Institute of Belgium, Brussels, Belgium
[2]Austrian Lightning Detection and Information System (ALDIS), Vienna, Austria
[3]Météorage, Pau, France
[4]Scientific Lightning Solutions LLC (SLS), Titusville, Florida, USA
[5]National Institute for Space Research, INPE, São José dos Campos, Brazil
[6]The Johannesburg Lightning Research Laboratory, School of Electrical and Information Engineering,
University of Witwatersrand, Johannesburg, Johannesburg, South Africa
[7]Institute of High Voltage Engineering and System Performance, Graz University of Technology, Graz, Austria
[8]ZT Research, Rapid City, South Dakota, USA

Correspondence: Dieter Poelman (dieter.poelman@meteo.be) and Wolfgang Schulz (w.schulz@ove.at)

Abstract. Information about lightning properties is important in order to advance the current understanding of lightning, whereby the characteristics of ground strike points (GSPs) are in particular helpful to improving the risk estimation for lightning protection. Lightning properties of a total of 1174 negative downward lightning flashes are analyzed. The high-speed video recordings are taken in different regions, including Austria, Brazil, South Africa and the USA, and are analyzed in terms of flash multiplicity, duration, interstroke intervals and ground strike point properties. According to our knowledge this is the first simultaneous analysis of GSP properties in different regions of the world applying a common methodology. Although the results vary among the data sets, the analysis reveals that a third of the flashes are single-stroke events, while the overall mean number of strokes per flash equals 3.67. From the video imagery an average of 1.56 GSPs per flash is derived, with about 60 % of the multiple-stroke flashes striking the ground in more than one place. It follows that a ground contact point is struck 2.35 times on average. Multiple-stroke flashes last on average 371 ms, whereas the geometric mean (GM) interstroke interval value preceding strokes producing a new GSP is about 18 % greater than the GM value preceding subsequent strokes following a pre-existing lightning channel.

In addition, a positive correlation between the duration and multiplicity of the flash is presented. The characteristics of the subset of flashes exhibiting multiple GSPs is further examined. It follows that strokes with a stroke order of 2 create a new GSP in 60 % of the cases, while this percentage quickly drops for higher-order strokes. Further, the possibility of forming a new lightning channel to ground in terms of the number of strokes that conditioned the previous lightning channel shows that approximately 88 % developed after the occurrence of only one stroke. Investigating the time intervals in the other 12 % of the cases when two or more strokes re-used the previous lightning channel showed that the average interstroke time interval preceding a new lightning channel is found to be more than twice the time difference between strokes that follow the previous lightning channel.

1 Introduction

Cumulonimbus clouds are the birthplace of one of Earth's true spectacles in nature: the lightning discharge. The development of these clouds involves a number of steps. As the building phase comes to an end, characterized by a rapid increase in growth of the clouds' height through the rise of

pockets of warm and moist air, it sets the stage for super-cooled cloud droplets to coagulate and increase in both mass and size. The subsequent mature phase provides the electric charge structure through a range of collisions between the icy particles. Typically, this results in the top of the cloud being predominantly positively charged, while the bottom of the cloud accommodates the bulk of the negatively charged particles. It is at this magical moment, when eventually the difference in charge potential reaches a certain threshold, that the cloud "switches on the light" and powerful electrical discharges appear, proudly drawing the attention of the spectator to an even greater extent than was the case moments before. Followed by the dissipation phase, this gigantic wasteland of energy, once capable of producing severe weather at the ground, disappears and leaves us in awe.

Lightning radiates its energy in almost the full range of the electromagnetic spectrum. Hence, to observe and further increase our understanding of lightning discharges in these cauliflower-like clouds and the associated forces and physical processes that are present within them, a whole range of instruments and techniques are at our disposal. The use of ground-based lightning location systems (LLSs), much in the same way compared to those constructed by today's standards, was first introduced more than 40 years ago (Lewis et al., 1960; Krider et al., 1976). Present-day LLSs operate from very low frequencies (VLFs) to very high frequencies (VHFs) and are able to detect cloud-to-ground (CG) strokes and intracloud (IC) pulses (e.g., Bürgesser, 2017; Said et al., 2010; Gaffard et al., 2008; Zhu et al., 2017; Murphy et al., 2021; Schulz et al., 2016; Coquillat et al., 2019). Depending on the adopted technique, the total pathway covered by a lightning flash can be presented as a single point or constitute several points (even up to thousands of points) for a single discharge. Modern ground-based low-frequency LLSs are capable of differentiating between CG and IC flashes and tend to perform well in terms of flash and stroke detection efficiencies, providing the location of downward CG ground strike points with high confidence.

On the other hand, satellite missions with dedicated on-board instruments provide a different way of capturing the stroboscopical dance of lightning discharges by observing the scattered light peaking through the top of the cloud. The signature of the strong optical oxygen triplet emission line at 777.4 nm is typically what is observed by means of specifically designed cameras. Although first attempts had already started in the 1970s (Vorpahl et al., 1970; Sparrow and Ney, 1971; Turman, 1978), one had to wait until 1995 with the launch of the OrbView 1 (MicroLab 1) satellite with the on-board Optical Transient Detector (OTD), closely followed by the Tropical Rainfall Measuring Mission (TRMM) carrying the Lightning Imaging Sensor (LIS) in 1997, to witness the potential and significance of that type of mission. While the latter satellites moved in a polar orbit around the Earth, the latest and future types of optical lightning instruments are being put into operation from a geostationary orbit (Goodman et al., 2013; Yang et al., 2017, Grandell et al., 2009), thereby expanding even further the range of associated applications.

Even though it is not uncommon to become lyrical about today's achievements in this field of research, the observations from ground-based LLSs as well as from space have, besides many advantages, one fundamental drawback as the lightning discharges are observed indirectly. By contrast, high-speed camera observations observe the light emitted directly by the lightning discharge, thereby documenting the flow of the electrically charged particles through the air, and provide, linked to electric field measurements, a means to investigate in great detail the associated optical and electromagnetic properties of natural downward lightning flashes. With frame rates of $200\,\text{s}^{-1}$ (fps) or more, the different strokes that compose a multi-stroke flash can each be captured individually, while it is the electric field measurement that undisputably identifies the polarity of each stroke. Furthermore, video imagery enables us to determine, if not too distant and/or obscured by precipitation, whether each individual stroke creates a new ground contact point (NGC) or follows a pre-existing lightning channel (PEC). The characteristics deduced from this are not only relevant from a pure scientific perspective but also essential in developing adequate lightning protection solutions as the level of lightning protection and risk to be mitigated is derived from the density of lightning terminations in a region. Typically, this is based on flash density values, but there have been recommendations to increase calculated densities by a factor of 2 to account for multiple ground strike point flashes (Bouquegneau, 2014; IEC 62858 Ed. 2, 2019). Understanding these characteristics is essential for evaluating whether such a factor is relevant.

In this paper, high-speed camera observations are analyzed in order to deduce some of the characteristics observed in natural negative downward lightning flashes. Section 2 describes briefly the instrumentation used per region, and analysis thereof is provided in Sect. 3. Section 4 summarizes the findings of this study. In this context, it is worthwhile mentioning that the data sets described here serve as basis to investigate the ability of so-called ground strike point algorithms to correctly group strokes in flashes according to the observed ground strike points (Poelman et al., 2021, companion paper).

2 Data acquisition and analysis

Ground-truth campaigns are time-consuming because enough data need to be gathered to be statistically relevant. To reach this objective, ground-truth data sets are collected from different geographical regions and taken over various periods in time: Austria (AT) in 2012, 2015, 2017 and 2018; Brazil (BR) in 2008; South Africa (SA) in 2017–2019; and the USA (US) in 2015.

Before going into more detail on the methods of data collection, it is of importance to recognize the limitations inherent to high-speed camera observations when used in flash characteristic studies. In particular, strokes creating a new termination could be missed by the camera when occurring out of the camera's field of view. In addition, the record length should be long enough to capture the entire flash, i.e., typically longer than 1 s. Aiming to minimize as much as possible the influence of the latter on the retrieved flash statistics, high-speed camera observations should be checked against concurrent electric field measurements to ensure a stroke was not missed. In this, flashes with lightning channels that are outside the field of view should be excluded from the data. For the measurements in all of the data sets presented in this study, electric field measurements have been used, and therefore only flashes where a clear visible lightning channel to the ground is observed for all the associated strokes are included. However, it should be noted that even though such a selection of flashes is made, it does not undeniably resolve the true contact point all of the time. This is certainly true when the observations are made at the ground level. As such, the number of ground strike points retrieved from the video measurements as discussed later on in this study should be regarded as a lower limit.

Finally, it is essential to remark that the flash grouping, i.e., grouping strokes belonging to the same flash, is based on the video images alone without any input from LLS data whatsoever. Clearly, it would make more sense to trace the lightning leader back to the location of the preliminary breakdown and only group strokes that emanate from a common charge region. However, this would require observations made by a lightning mapping array.

In what follows, a description is given of the instrumentation setup used in the different regions and the periods of investigation.

2.1   Austria

A so-called video and field recording system (VFRS) is used to document lightning strikes in the alpine region of Austria. The VFRS consists of a high-speed camera and an electric field measurement system, and both are GPS time synchronized. The system is composed of a flat-plate antenna, an integrator and an amplifier, a fiber optic link, a digitizer, and a PXI system (Schulz et al., 2005). The camera used for the data recorded in 2015, 2017 and 2018 is the Vision Research Phantom v9.1, operated at a frame rate of 2000 fps, a 14 bit image depth and a resolution of 1248×400 pixels (Schulz and Saba, 2009; Vergeiner et al., 2016; Schwalt, 2019; Schwalt et al., 2020) with a total record length of 1.6 s. In 2012 a monochrome (8 bit per pixel) Basler camera was used at 200 fps with a VGA resolution, i.e., 640×480 pixels, and with a record length of 5 s.

2.2   Brazil

A Photron 512 PCI high-speed digital camera, operating at 4000 fps, was used to record the flashes in southeastern Brazil in 2008. The high-speed video images are GPS time-stamped to an accuracy of better than 1 ms with a 1 s pre-trigger time and a total recording time of 2 s. Each trigger pulse was initiated manually by an operator when a flash was observed within the camera field of view. For more details on the operation and accuracy of high-speed cameras for lightning observations, see Saba et al. (2016). The polarity of the strokes is determined by matching the strokes to electric field measurements and to the observations of a local lightning location system BrasilDat in Brazil. More information on the characteristics of this network is given by Naccarato and Pinto (2009).

2.3   South Africa

The high-speed study of lightning flashes over Johannesburg, South Africa, began in 2017. Johannesburg is located in the northeastern province of Gauteng and sits at an altitude of approximately 1600 m a.s.l. The area has seasonal thunderstorms, generally occurring during the middle-to-late afternoons in the summer months (September–April, Southern Hemisphere) and with no thunderstorm activity during the winter months. The area has a flash density of 15 to 18 flashes km^{-2} yr^{-1} (Evert and Gijben, 2017). The setup utilizes two high-speed cameras (a Phantom v7.1 and a Phantom v310) which are located northwest of the city. Frame rates used are in the range of 5000 to 15000 fps, and all captured videos are GPS time-stamped. A 1.8 s buffer time is used and events are manually triggered. Typically, the pre-trigger and post-trigger were set at approximately 60 % and 40 % of the 1.8 s buffer, respectively. Note that in this area both downward and upward lightning discharges are captured. The latter are events triggered by the two tall towers located in Johannesburg – the Sentech and Hillbrow towers – each approximately 250 m high (Schumann et al., 2018). However, all tower events in the SA data set are excluded from the analysis in this study.

2.4   USA

The observations used in this study are taken from the Kennedy Space Center and Cape Canaveral Space Force Station (KSC–CCSFS) in 2015 (Hill et al., 2016). A compact network of 13 high-speed cameras record cloud-to-ground lightning return strokes terminating on KSC–CCSFS property, with geographic emphasis on the areas surrounding Launch Complex 39B (LC-39B), Launch Complex 39A (LC-39A), Launch Complex 41 (LC-41) and the Vehicle Assembly Building (VAB). Eight of the cameras are located on tall structures at altitudes greater than 150 m, providing downward vantage points. Many of the cameras are configured

Table 1. Flash characteristics.

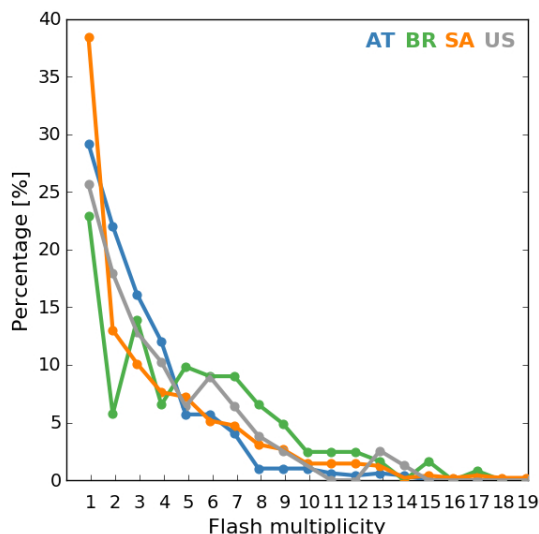| Parameter	Location ground-truth observations				
	AT	BR	SA	US	All
N (flashes)	490	122	484	78	1174
N (strokes)	1539	619	1839	305	4302
Mean multiplicity	3.14	5.07	3.8	3.90	3.67
Max multiplicity	14	17	26	14	26
Percentage of single-stroke flashes	29.2	23.0	38.4	25.6	32.1
N (GSPs)	845	232	626	129	1832
Average N (GSPs per flash)	1.72	1.90	1.29	1.65	1.56
Max N (GSPs per flash)	5	4	5	4	5
Average N (strokes per GSP)	1.82	2.67	2.94	2.36	2.35
Average flash duration[a,b] (ms)					
All flashes	233	415	262	236	264
Multiple-stroke flashes	306	538	394	328	371
Occurrence of forked strokes[c]					
Percentage of flashes containing at least one forked stroke	9.4	10.7	7.0	10.3	8.3
Percentage of forked strokes in flashes containing at least one forked stroke	34.4	21.8	20.8	42.8	24.1
Percentage of forked strokes in the overall data set	3.7	2.3	2.2	2.9	2.5
Continuing current (CC)					
Mean (ms)	67.1	36.5	38.5	–	44.5
Median (ms)	15.0	8.0	9.0	–	10.0
Max (ms)	540	705	929	–	929
Percentage of strokes followed by CC $\geq$ 3 ms	33.7	71.7	73.0	–	57.7
Percentage of strokes followed by CC $\geq$ 500 ms	0.26	0.32	0.38	–	0.33
Percentage of flashes containing CC $\geq$ 10 ms	37.8	61.5	61.8	–	51.0

[a] Flash duration is defined as the time interval between the occurrence of the first return stroke and the end of the continuing current following the last return stroke if present. [b] Values for US do not include continuing-current duration. [c] For AT only, based on data taken in 2018.

with intersecting fields of view to provide multi-angle scenes of the same discharge. The high-speed cameras sample at either 3200 or 16 000 fps. The cameras have memory segment lengths ranging from about 100 to 400 ms and operate in segmented memory mode in order to capture many consecutive events without overrunning the internal buffer. In this way, the entire sequence of strokes is captured over the full duration of a flash. In addition, six wideband rate of change in electric field (dE/dt) sensors provide information on the polarity of the discharges. The digitization time bases of these geographically independent sensors are synchronized with rms accuracy of 15 ns.

3　Results

The combined data sets comprise 1174 flashes and 4302 strokes. The characteristics of each individual data set regarding flashes, strokes, ground strike points, forked stroke occurrence, multiplicity, flash duration and length of the continuing current (CC) are presented in Table 1. The largest data set in terms of number of flashes is the one of Aus-
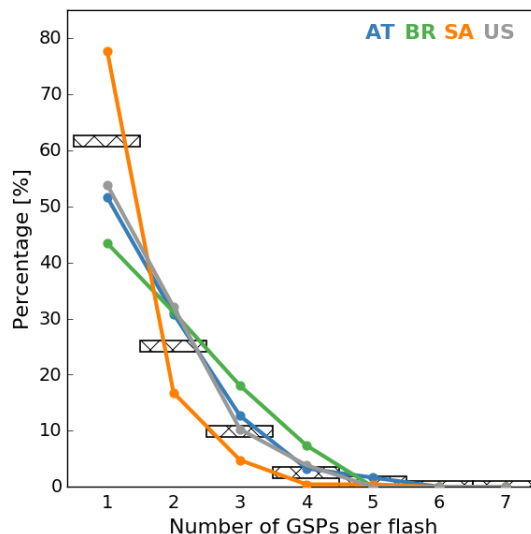
tria with 490 flashes, closely followed by the South African data set containing 484 flashes. On the other hand, the data set of South Africa includes by far the largest number of strokes. The distribution of the flash multiplicity of the individual data sets is depicted in Fig. 1. Clearly, the flash multiplicity depends on the ability to identify all the respective strokes that occurred during the flash. The video frame rates listed in the previous section that were used for the observations are believed to be more than sufficient to meet this requirement. Mean flash multiplicities range from 3.14 (AT) to 5.07 (BR) strokes per flash, with an observed overall combined flash multiplicity of 3.67. The multiplicities in this study are in line with average multiplicity values published in other studies such as Rakov et al. (1994), Cooray and Perez (1994), Cooray and Jayaratne (1994), Saba et al. (2006), and Saraiva et al. (2010) and lower than what was found by Ballarotti et al. (2012) and Kitagawa et al. (1962). From Fig. 1 and Table 1 it can be seen that the percentage of single-stroke flashes varies between 23 % (BR) and 38.4 % (SA), with an average of 32.1 % for all the flashes combined. One could argue that the latter percentages are somewhat higher compared to those quoted in well-known reports of

Figure 1. Distribution of the number of strokes per flash.

Figure 2. Distribution of the number of GSPs per flash. The shaded rectangles represent the result for the combined data sets.

accurate stroke count studies such as the 13 % observed in New Mexico by Kitagawa et al. (1962), 17 % in Florida by Rakov and Uman (1990), 18 % in Upssala by Cooray and Pérez (1994), and 21 % in Sri Lanka as described in Cooray and Jayaratne (1994). Nonetheless, the 29.2 % retrieved for AT in this study is comparable to the 27 % analyzed in detail by Schwalt et al. (2021), which, in addition, also demonstrated that the percentage of single-stroke flashes can vary considerably from one storm to another without an apparent dependency on thunderstorm type or underlying meteorological characteristics. The 23 % of single-stroke flashes for BR in the present study is only a few percent higher than the 17 % observed within the São Paolo state retrieved by Ballarotti et al. (2012). In the case of SA, there exist no previously published values of single-stroke occurrences against which to check the 38.4 %. It seems that this area, at an altitude of about 1600 m a.s.l., is prone to single-stroke flashes. The origin of this discrepancy, compared to the other regions, is indeed worth a thorough investigation but is out of the scope of this particular study. Finally, Fleenor et al. (2009) found that 40 % of the negative cloud-to-ground flashes are single-stroke flashes observed in the US Central Great Plains. It was noted that the time resolution of the camera was limited to 16.7 ms, which could lead to an underestimation of the true negative multiplicity by about 11 % (Biagi et al., 2007). However, even taking this underestimation into account, the percentage of the single-stroke flashes in Fleenor et al. (2009) is higher than the value in this study for US. The value of the maximum multiplicity per data set is indicated in Table 1 as well. One flash in SA stands out, containing a total of 26 strokes while lasting 1.06 s.

As mentioned earlier, video observations allow classification of each stroke as a discharge either creating a new ground strike point (GSP) or following a PEC. As such, a to-

tal of 1832 GSPs are resolved within the different data sets; yielding an average of 1.56 GSPs per flash, while the mean number of GSPs per flash for the different data sets ranges from 1.3 (SA) to 1.9 (BR). It follows that the average number of lightning strike points is 56 % higher than the number of flashes. This value is in line with those reported in earlier studies such as the 1.45 strike points per CG flash observed in Tucson, Arizona, by Valine and Krider (2002) and 1.67 strike points per flash in Florida (Rakov et al., 1994), while in São Paulo, Brazil, and in Arizona, USA, a value of 1.70 was retrieved (Saraiva et al., 2010). The distribution of the number of GSPs per flash for the different data sets is plotted in Fig. 2. SA is the data set containing the highest number of flashes with a single GSP percentage-wise. This is a consequence of the number of single-stroke flashes observed in SA. In total, about 62 % of the flashes strike the ground at only one point. However, this value drops to 44 % when single-stroke flashes are excluded. In other words, the majority (56 %) of multiple-stroke negative downward flashes strike the ground in more than one place. The maximum number of GSPs in a flash is found to be five, observed in Austria as well as in South Africa. Finally, adopting the values in Table 1 for the multiplicity and average number of strike points for each data set, the average number of strokes observed per GSP varies between 1.82 (AT) and 2.94 (SA). For all the data sets combined it turns out that a ground contact point is struck 2.35 times on average.

Forked strokes, i.e., strokes wherein the lightning channel towards the ground branches off, are an additional source of ground contact points. The occurrence of such strokes within each data set is indicated in Table 1. Averaged over all the data sets, it is found that 8.3 % of the observed flashes comprise at least one forked stroke. Examining those latter
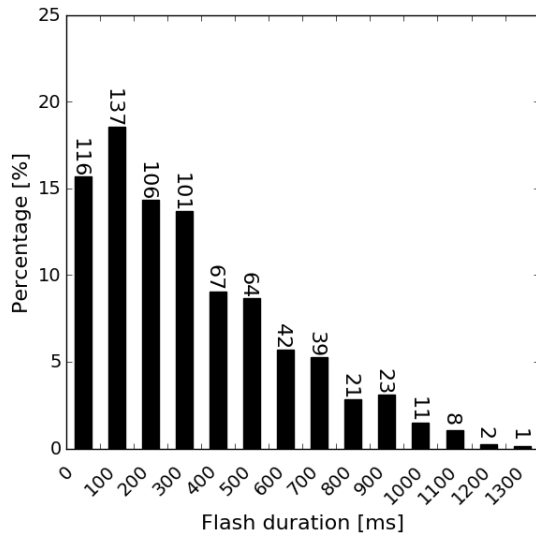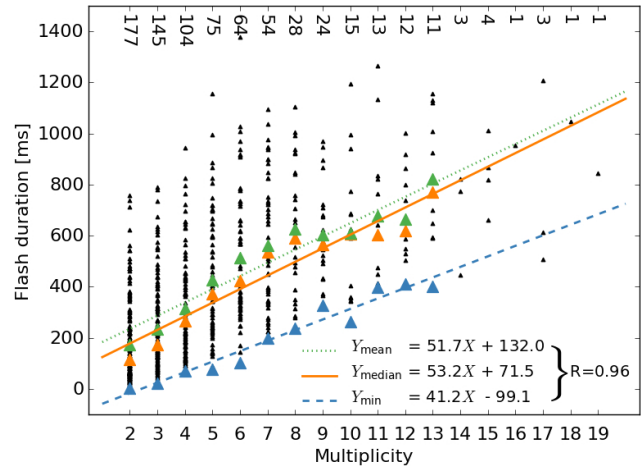
Figure 3. Distribution of the flash duration in bins of 100 ms. The actual number of flashes within each bin is listed above the bars.


Figure 4. Distribution of the flash duration as a function of multiplicity. The equation for the minimum, median and mean regression is given as well as the correlation coefficient of 0.96, being similar for all three regressions. The actual number of flashes per multiplicity is indicated at the top of the plot.

flashes that contain one or more forked strokes, 24.1 % of the strokes within those flashes are forked, whereas overall this is only the case in 2.5 % of all observed strokes in this study. If one were to apply a percentage associated with the individual data sets of the observed strokes that are forked, this would result in an increase in the average number of ground strike points per flash, N (GSPs per flash), as indicated in Table 1, by this same factor.

Since the duration of a flash is defined as the time span between the first and last stroke in the flash, increased by the duration of an eventual continuing current following the last stroke, it is worthwhile to further highlight the occurrence and specifics of CCs. Following the approach as in Ballarotti et al. (2012), a 3 ms minimum CC duration is applied in order to eliminate what could just be return-stroke pulse tails in the high-speed camera records. Considering all ranges of CCs ($\geq$ 3 ms), the mean CC duration ranges from 38.5 ms in SA up to 67.1 ms as observed in AT, with an overall average of 44.5 ms. Median values are considerably lower with an overall median of 10 ms. The maximum value of 929 ms was measured in South Africa, which is about 200 ms longer than the maximum value found in Ballarotti et al. (2012). Out of 1096 flashes recorded with CC information, 51 % contained continuing currents with a duration greater than 10 ms and 57.7 % of all strokes were followed by a CC greater than 3 ms. Only a small portion, i.e., 0.33 %, of the strokes are followed by a CC longer than 500 ms.

Figure 3 illustrates the duration of all the flashes in bins of 100 ms. Since the US data set does not contain information on the possible occurrence of CC, the plot is made excluding US flashes. In addition, only multiple-stroke flashes are included since many of the single-stroke flashes were not followed by any CC, therefore influencing the percentage of

flashes that fall into the first duration bin. The mean and median duration of multiple-stroke flashes is found to be 371 and 313 ms, respectively. Of the flashes, 95 % have a duration below 926 ms. The flash with the longest duration of 1379 ms is observed in SA for a six-stroke flash and is in line with the maximum flash duration values found in Saba et al. (2006) and Ballarotti et al. (2012).

One can intuitively suppose that with increasing flash multiplicity, the flash duration increases accordingly. While this is in general true, a large spread is observed in the data. This becomes apparent in Fig. 4, which plots the flash duration as a function of multiplicity. Note that for instance in SA the maximum flash duration is found for a flash with a multiplicity of 6. Additionally, Fig. 4 indicates the regression slope based on the minimum, median and mean flash duration values per multiplicity. For this purpose, only multiplicities up to a value of 13 are taken into account since the sample size becomes too low at higher multiplicities. The regression equations, as well as the correlation coefficient, R, are indicated in the figure. The equations for the minimum and mean flash duration in this study compared to those presented in Saraiva et al. (2010) and Ballarotti et al. (2012) have a lower slope by a factor of 1.5 and 1.2, respectively.

Figure 5 displays the percentage of subsequent strokes creating a new GSP as a function of stroke order, based on a total of 658 new GSPs from the combined data sets. While a stroke with a stroke order of 2, i.e., the first subsequent stroke in the flash, still creates a new GSP in 60 % of the cases, this quickly drops to 25 % and 10 % for the third and fourth stroke in the flash, respectively. Those values are comparable to the values presented in Stall et al. (2009). On the other hand, although following a similar decreasing trend, the average per-
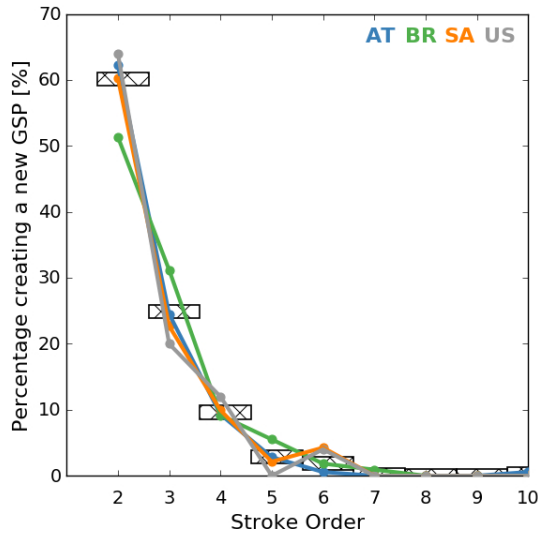
Figure 5. Distribution of the percentage of subsequent strokes creating a new GSP as a function of stroke order. The shaded rectangles represent the result for the combined data sets.
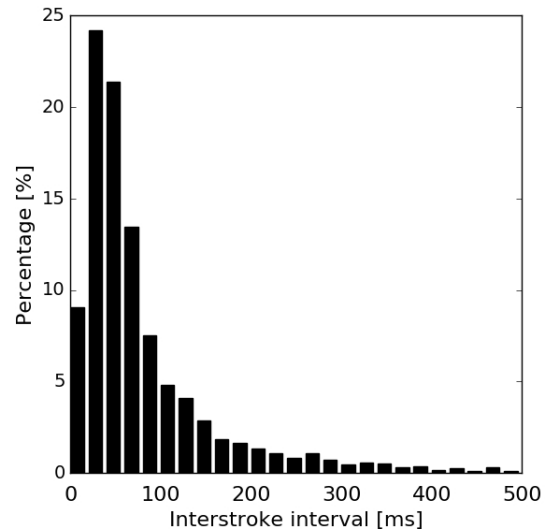
Figure 7. Interstroke time intervals for all subsequent strokes and for the same and new lightning channels.
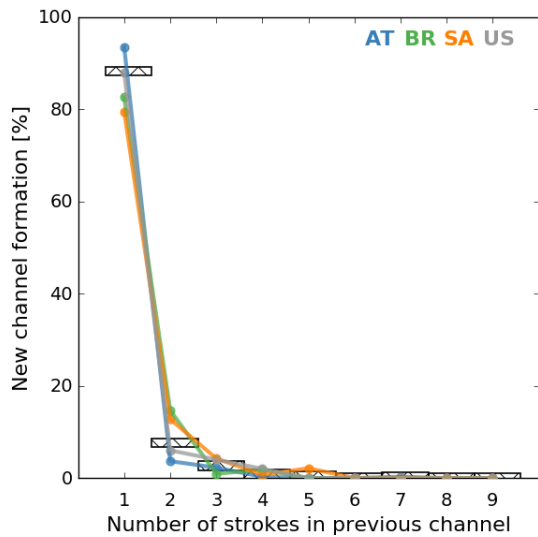
Figure 6. Relation between new lightning channel formation and the number of strokes in previous lightning channel. The shaded rectangles represent the result for the combined data sets.

centage found in this study for a stroke with a stroke order of 2 in the flash is higher by about 10 %–20 % compared to what has been found previously in Rakov et al. (1994), Saba et al. (2006) and Ferro et al. (2012).

It has been suggested by Rakov and Uman (1990) that the conditions after the first stroke in the flash are not favorable to fully supporting the propagation of subsequent leaders all the way to the ground along the same path. Therefore, the stroke order alone is not sufficient to predict the chance of creating a new GSP, as the full lightning channel history needs to be taken into account. The possibility of forming

a new lightning channel to ground as a function of the number of strokes that conditioned the previous lightning channel is quantified in Fig. 6. Out of a total of 658 new lightning channels, 88.2 % developed after the occurrence of only one stroke, while this drops quickly to 7.6 % and 2.6 % in case of two and three observed consecutive strokes, respectively, in the previous lightning channel. Note that in Austria two flashes are observed whereby a new GSP is created by the 10th stroke in the flash while the lightning channel belonging to the previous GSP was used four and seven times, respectively. In the latter case, this indicates that even after seven consecutive strokes within the same lightning channel, it is still possible that the conditions to establish an unalterable path to ground are not met or are simply ignored by a subsequent stroke. According to Ferro et al. (2012), when two or more strokes have used the previous lightning channel, then a larger interstroke time interval may be an important factor in the creation of a new lightning channel. While the interstroke time intervals will be discussed in more detail later on, it is worthwhile to point out that the interstroke time intervals between the 9th and 10th stroke in case of the two Austrian flashes as mentioned above are 26.2 and 103.97 ms, respectively.

The distribution of 3128 time intervals is plotted in Fig. 7 adopting a bin size of 20 ms, and results thereof are listed in Table 2. The average time interval is 85 ms, with a geometric mean (GM) of 57 ms. The maximum time interval for the individual data sets is on the order of 500 to 700 ms, except for SA which contains a six-stroke flash with a maximum observed time interval of 905 ms between the fifth and last stroke in the flash. Note that this particular flash is also the flash with the maximum flash duration in all the data sets and can be regarded as an exception, although time intervals well

Table 2. Statistics for interstroke time intervals that precede subsequent PEC and NGC.

	AT		BR		SA		US		All		
	N^a	GM [ms]	N	GM [ms]	N	GM [ms]	N	GM [ms]	N	GM [ms]	SE^b [ms]
ΔT_{PEC}	662	62	362	68	1199	49	162	52	2385	55	1.8
ΔT_{NGC}	351	56	108	64	133	93	42	73	634	65	3.9
ΔT_{All}	1013	60	470	67	1332	52	204	57	3019	57	1.6

[a] N is sample size. [b] SE is standard error.

Table 3. Interstroke time interval between strokes using a PEC and interstroke time interval preceding an NGC after two or more strokes down the same lightning channel.

	AT		BR		SA		US		Combined	
	N^a	[ms]	N	[ms]	N	[ms]	N	[ms]	N	[ms]
PEC	38	31	24	44	56	32	10	31	128	34
SE^b [ms]		8.8		6.2		5.5		6.4		3.8
NGC	23	68	19	67	29	86	6	113	77	77
SE [ms]		15.3		15.6		33.7		19.2		14.4

[a] N is sample size. [b] SE is standard error.

exceeding 500 ms are recorded in other studies, e.g., Saba et al. (2006). Usually, these long time intervals between strokes are due to a very long continuing-current event following the first one. The 99th percentile appears to be 470 ms, somewhat below the standard maximum interstroke time criterion of 500 ms usually adopted to group different strokes into flashes by lightning location systems.

It is possible to further separate the interstroke time intervals from Fig. 7 into intervals preceding strokes down the same lightning channel, ΔT_{PEC}, or down a new lightning channel, ΔT_{NGC}. The results of this can be viewed in Table 2 for the individual data sets, as well as for all the data sets combined. Overall, it is found that the GM for ΔT_{NGC} is slightly larger compared to ΔT_{PEC} by 10 ms. While Rakov et al. (1994) found a larger difference between ΔT_{NGC} and ΔT_{PEC}, this was probably due to the limited sample size involved. Subsequent follow-up studies by, e.g., Saba et al. (2006) and Ferro et al. (2012), showed that the GM values of ΔT_{NGC} and ΔT_{PEC} converge towards each other while adopting a larger data set, as is the case in this study.

There are some noticeable differences among the individual data sets. While it is clear that ΔT_{NGC} is considerably larger than ΔT_{PEC} in SA and US, the differences are much smaller or the opposite in the other data sets.

Some further investigation with respect to the time differences, analogous to Ferro et al. (2012), is presented in the following. From Fig. 6 it is found that in 88 % of the cases a new lightning channel formation is observed after just one stroke in the previous lightning channel. Investigating now the time intervals in the other 12 % of the cases when two or more strokes re-used the previous lightning channel, we find

that the average interstroke time interval preceding a new lightning channel becomes 77 ms, compared to a time difference of 34 ms between strokes that follow the same lightning channel; see Table 3. Therefore, in this subset of flashes, ΔT_{NGC} is about 2.3 times larger compared to ΔT_{PEC}. This value is somewhat lower compared to the 3.5 times found in Ferro et al. (2012) but still of the same order. Note that the interstroke time interval GM value for PEC strokes is in this case lower by a factor of 1.6 compared to the result in Table 2.

4 Summary

Ground strike point characteristics in negative ground lightning flashes have been investigated by means of high-speed camera observations made in different places around the globe. According to our knowledge this is the first simultaneous analysis of GSP properties in different regions of the world applying a common methodology. It is found that the mean number of ground strike points per flash is 1.56, varying in the four regions from 1.29 to 1.90. The maximum number of GSPs per flash just fluctuates between 4 and 5, while the mean number of strokes per GSP ranges from 1.82 to 2.94. From this, it follows that the ground strike point statistics differ in different regions. The values quoted in this study are in line with those found in the literature and reconfirms the necessity to take ground strike points into account to estimate the risk for lightning protection purposes. While the number of flashes and strokes involved in this study is statistically relevant and, above all, larger compared to any

other similar study undertaken in the past, it remains a snapshot of that particular moment in time and place. Consequently, more detailed investigation of the regional and seasonal trends that might exist is required. In order to overcome this, one could make use of the observations made by LLSs. Present-day LLSs provide, with a high degree of accuracy in terms of both efficiency and location, the different strokes that compose a flash. Ingesting those observations into a so-called ground strike point algorithm, in order to group individual strokes into ground strike points, would provide a means to study the characteristics of ground strike point densities on a larger temporal and spatial scale. The interested reader is referred to Poelman et al. (2021, companion paper) to learn more about the ability of three such algorithms to determine the observed ground strike points correctly based on the data set presented in this study.

The 99th percentile of the interstroke intervals is found to be 470 ms and certifies the commonly used maximum interstroke interval of 500 ms to group strokes observed by an LLS into a flash while adopting a certain distance threshold. In addition, it follows that the GM value for time intervals preceding the occurrence of a new lightning channel is only slightly larger than the typical GM interstroke interval value of 57 ms. Overall, apart from a few exceptions, the total flash duration is below 1 s and exhibits a positive correlation with the flash multiplicity.

In the majority of the cases, i.e., 88 %, a new lightning channel formation is observed after just one stroke in the previous lightning channel. This fact, together with the almost similar interstroke time intervals preceding strokes producing an NGC or following a PEC, suggests that time interval alone is not enough to influence the creation of a new lightning channel to ground. However, examining the cases when two or more strokes re-used the previous lightning channel, the average interstroke time interval preceding a new lightning channel is more than double the interval time between previous strokes that follow the same lightning channel. This analysis strengthens the outcome of Ferro et al. (2012).

References

Ballarotti, M. G., Medeiros, C., Saba, M. M. F., Schulz, W., and Pinto Jr., O.: Frequency distributions of some parameters of negative downward lightning flashes based on accurate-stroke-count studies, J. Geophys. Res., 117, D06112, https://doi.org/10.1029/2011JD017135, 2012.

Biagi, C. J., Cummins, K. L., Kehoe, K. E., and Krider, E. P.: National Lightning Detection Network (NLDN) performance in southern Arizona, Texas, and Oklahoma in 2003–2004, J. Geophys. Res., 112, D05208, https://doi.org/10.1029/2006JD007341, 2007.

Bouquegneau, C.: The need for an international standard on Lightning Location Systems, in: 23rd International Lightning Detection Conference, 18–19 March 2014, Tucson, Arizona, USA, 2014.

Bürgesser, R. E.: Assessment of the World Wide Lightning Location Network (WWLLN) detection efficiency by comparison to the Lightning Imaging Sensor (LIS), Q. J. Roy. Meteor. Soc., 143, 2809–2817, https://doi.org/10.1002/qj.3129, 2017.

Cooray, V. and Jayaratne, K. P. S. C.: Characteristics of lightning flashes observed in Sri Lanka in the tropics, J. Geophys. Res., 99, 21051–21056, https://doi.org/10.1029/94JD01519, 1994.

Cooray, V. and Pérez, H.: Some features of lightning flashes observed in Sweden, J. Geophys. Res., 99, 10683–10688, https://doi.org/10.1029/93JD02366, 1994.

Coquillat, S., Defer, E., de Guibert, P., Lambert, D., Pinty, J.-P., Pont, V., Prieur, S., Thomas, R. J., Krehbiel, P. R., and Rison, W.: SAETTA: high-resolution 3-D mapping of the total lightning activity in the Mediterranean Basin over Corsica, with a focus on a mesoscale convective system event, Atmos. Meas. Tech., 12, 5765–5790, https://doi.org/10.5194/amt-12-5765-2019, 2019.

Evert, R. C. and Gijben, M.: Official South African Lightning Ground Flash Density Map 2006 to 2017 – Earthing Africa Inaugural Symposium and Exhibition, Johannesburg, South Africa, 2017.

Ferro, M. A., Saba, M. M. F., and Pinto Jr., O.: Time intervals between negative lightning strokes and the creation of new ground terminations, Atmos. Res., 116, 130–133, 2012.

Fleenor, S. A., Biagi, C. J., Cummins, K. L., Krider, E. P., and Shao, X.: Characteristics of cloud-to-ground lightning in warm-season thunderstorms in the Central Great Plains, Atmos. Res., 91, 333–352, 2009.

Gaffard, C., Nash, J., Atkinson, N., Bennett, A., Callaghan, G., Hibbett, E., Taylor, P., Turp, M., and Schulz, W.: Observing lightning around the globe from the surface, in: 20th International Lightning Detection Conference, Tucson, Arizona, USA, 21–23, 2008.

Goodman, S. J., Blakeslee, R. J., Koshak, W. J., Mach, D., Bailey J., Buechler, D., Carey, L., Schultz, C., Bateman, M., McCaul, E., and Stano, G.: The GOES-R Geostationary Lightning Mapper (GLM), Atmos. Res., 125–126, 34–49, 2013.

Grandell, J., Finke, U., and Stuhlmann, R.: The EUMETSAT meteosat third generation lightning imager (MTG-LI): Applications and product processing, in: Proceedings of the 9th EMS Annual Meeting, 28 September–2 October 2009, Toulouse, France, 2009.

Hill, J. D., Mata, C. T., Nag, A., and Roeder, W. P.: Evaluation of the performance characteristics of MERLIN and NLDN based on two years of ground-truth data from Kennedy Space Center/Cape Canaveral Air Force station, Florida, in: 24th International Lightning Detection Conference, San Diego, California, USA, 2016.

International Standard: IEC 62858, Edition 2, lightning density based on lightning location systems (LLS) – General principles, International Electrotechnical Commission, ISBN 978-2-8322-7457-6, 2019.

Kitagawa, N., Brook, M., and Workman, E. J.: Continuing currents in cloud-to-ground lightning discharges, J. Geophys. Res., 67, 637–647, https://doi.org/10.1029/JZ067i002p00637, 1962.

Krider, E. P., Noggle, R. C., and Uman, M. A.: A gated wide-band magnetic direction finder for lightning return strokes, J. Appl. Meteorol., 15, 301–306, 1976.

Lewis, E. A., Harvey, R. B., and Rasmussen, J. E.: Hyperbolic direction finding with sferics of transatlantic origin, J. Geophys. Res., 65, 1879–1905, 1960.

Murphy, M. J., Cramer, J. A., and Said, R. K.: Recent History of Upgrades to the U.S. National Lightning Detection Network, J. Atmos. Ocean. Tech., 38, 573–585, 2021.

Naccarato, K. P. and Pinto Jr., O.: Improvements in the detection efficiency model for the Brazilian lightning detection network (Brasil – DAT), Atmos. Res., 91, 546–563, https://doi.org/10.1016/j.atmosres.2008.06.019, 2009.

Poelman, D. R., Schulz, W., Pedeboy, S., Campos, L. Z. S., Matsui, M., Hill, D., Saba, M., and Hunt, H.: Global ground strike point characteristics in negative downward lightning flashes – Part 2: Algorithm validation, Nat. Hazards Earth Syst. Sci., 21, 1921–1933, https://doi.org/10.5194/nhess-21-1921-2021, 2021.

Rakov, V. A. and Uman, M. A.: Some properties of negative cloud-to-ground lightning, paper presented at 20th International Conference on Lightning Protection, Swiss Electrotechn. Assoc., Interlaken, Switzerland, 1990.

Rakov, V. A., Uman, M. A., and Thottappillil, R.: Review of lightning properties from electric field and TV observations, J. Geophys. Res., 99, 10745–10750, https://doi.org/10.1029/93JD01205, 1994.

Saba, M. M. F., Ballarotti, M. G., Pinto Jr., O.: Negative cloud-to-ground lightning properties from high-speed video observations, J. Geophys. Res. 111, D03101, https://doi.org/10.1029/2005JD006415, 2006.

Saba, M. M. F., Schumann, C., Warner, T. A., Ferro, M. A. S., de Paiva, A. R., Helsdon Jr., J., and Orville, R. E.: Upward lightning flashes characteristics from high-speed videos, J. Geophys. Res. Atmos., 121, 8493–8505, https://doi.org/10.1002/2016JD025137, 2016.

Said, R. K., Inan, U. S., and Cummins, K. L.: Long-range lightning geolocation using a VLF radio atmospheric waveform bank, J. Geophys.Res., 115, D23108, https://doi.org/10.1029/2010JD013863, 2010.

Saraiva, A. C. V., Saba, M. M. F., Pinto, O., Cummins, K. L., Krider, E. P., and Campos, L. Z. S.: A comparative study of negative cloud-to-ground lightning characteristics in São Paulo (Brazil) and Arizona (United States) based on high-speed video observations, J. Geophys. Res., 115, D11102, https://doi.org/10.1029/2009JD012604, 2010.

Schulz, W. and Saba, M. M. F.: First results of correlated lightning video images and electric field measurements in Austria, in: SIPDA, 9–13 November 2009, Curitiba, Brazil, 2009.

Schulz, W., Lackenbauer, B., Pichler, H., and Diendorfer, G.: LLS data and correlated continuous E-field measurements, in: SIPDA, 21–25 November 2009, Sao Paulo, Brazil, 2005.

Schulz, W., Diendorfer, G., Pedeboy, S., and Poelman, D. R.: The European lightning location system EUCLID – Part 1: Performance analysis and validation, Nat. Hazards Earth Syst. Sci., 16, 595–605, https://doi.org/10.5194/nhess-16-595-2016, 2016.

Schumann, C., Hunt, H. G. P., Tasman, J., Fensham, H., Nixon, K. J., Warner, T. A., and Saba, M. M. F.: High-speed Video Observation of Lightning Flashes Over Johannesburg, in: South Africa 2017–2018 International Conference on Lightning Protection, 2–7 September 2018, Rzeszow, Poland, 2018.

Schwalt, L.: Lightning Phenomena in the Alpine Region of Austria, PhD thesis, Graz University of Technology, 147 pp., 2019.

Schwalt, L., Pack, S., and Schulz, W.: Ground truth Data of Atmospheric Discharges in Correlation with LLS Detections, Elect. Pow. Syst. Res., 180, 106065, https://doi.org/10.1016/j.epsr.2019.106065, 2020.

Schwalt, L., Pack, S., Schulz, W., and Pistotnik, G.: Percentage of single-stroke flashes related to different thunderstorm types, Elect. Power Syst. Res., 194, 107109, https://doi.org/10.1016/j.epsr.2021.107109, 2021.

Sparrow, J. G. and Ney, E. P.: Lightning observations by satellite, Nature, 232, 514–540, 1971.

Stall, C. A., Cummins, K. L., Krider, E. P., and Cramer, J. A.: Detecting multiple ground contacts in cloud-to-ground lightning flashes, J. Atmos. Ocean. Tech., 26, 2392–2402, 2009.

Turman, B. N.: Analysis of lightning data from the DMSP satellite, J. Geophys. Res.-Oceans, 83, 5019–5024, https://doi.org/10.1029/JC083iC10p05019, 1978.

Valine, W. and Krider, E. P.: Statistics and characteristics of cloud-to-ground lightning with multiple ground contacts, J. Geophys. Res., 107, 4441, https://doi.org/10.1029/2001JD001360, 2002.

Vergeiner, C., Pack, S., Schulz, W., and Diendorfer, G.: Negative cloud-to-ground lightning in the alpine region: a new approach, in: CIGRE International Colloquium, 28–30 March 2016, Curitiba, Brazil, 2016.

Vorpahl, J. A., Sparrow, J. G., and Ney, E. P.: Satellite observations of lightning, Science, 169, 860–862, 1970.

Yang, J., Zhang, Z., Wei, C., Lu, F., and Guo, Q.: Introducing the new generation of Chinese geostationary weather satellites, Fengyun-4, B. Am. Meteorol. Soc., 98, 1637–1658, 2017.

Zhu, Y., Rakov, V. A., Tran, M. D., Stock, M. G., Heckman, S., Liu, C., Sloop, C. D., Jordan, D. M., Uman, M. A., Caicedo, J. A., Kotovsky, D. A., Wilkes, R. A., Carvalho, F. L., Ngin, T., Gamerota, W. R., Pilkey, J. T., and Hare, B. M.: Evaluation of ENTLN performance characteristics based on the ground truth natural and rocket-triggered lightning data acquired in Florida, J. Geophys. Res.-Atmos., 122, 9858–9866, https://doi.org/10.1002/2017JD027270, 2017.